

Strong gravitational lensing by braneworld black holes

Richard Whisker*

Institute for Particle Physics Phenomenology, University of Durham, South Road, Durham DH1 3LE, United Kingdom
(Received 16 December 2004; published 3 March 2005)

In this paper, we use the strong field limit approach to investigate the gravitational lensing properties of braneworld black holes. Applying this method to the supermassive black hole at the center of our galaxy, the lensing observables for some candidate braneworld black hole metrics are compared with those for the standard Schwarzschild case. It is found that braneworld black holes could have significantly different observational signatures to the Schwarzschild black hole.

DOI: 10.1103/PhysRevD.71.064004

PACS numbers: 04.50.+h, 04.70.Bw, 95.30.Sf, 98.62.Sb

I. INTRODUCTION

The braneworld paradigm provides an interesting framework within which to explore the possibility that our Universe lives in a fundamentally higher dimensional spacetime. Unlike the Kaluza-Klein picture where the extra dimensions must be compactified on a length scale $R \lesssim 10^{-17}$ cm in order to evade our detection, confinement of the standard model fields to a 3-brane, with only gravity propagating in the bulk, allows large, and even infinite, extra dimensions.

Recent work on braneworlds was instigated by the proposals of Arkani-Hamed, Dimopoulos and Dvali (ADD) [1] and Randall and Sundrum (RS) [2] (see [3] for early work, and [4] for braneworld reviews). The ADD model has n flat, compact extra dimensions of size R . Because of the confinement of ordinary matter to a brane, R can be as large as ~ 0.1 mm (the scale down to which Newton's law has been experimentally tested), and the model provides a possible resolution to the hierarchy problem if $n \geq 2$. More interesting from the general relativity viewpoint are the RS models proposed shortly afterwards. They allowed the bulk geometry to be curved, and endowed the branes with a tension. Their first model consisted of two branes of equal but opposite tension bounding a slice of anti-de Sitter (AdS) space. This model also gives a possible resolution to the hierarchy problem, provided we live on the negative tension brane. In their second model, RS considered a single, positive tension brane in an *infinite* bulk. This model, which is loosely motivated by string theory [5], has been one of the most popular to explore, and is the one we will be using.

Even though the extra dimension is infinite and gravity is inherently five dimensional, RS showed that the Newtonian potential of a particle on the brane was indeed the 4D $1/r$ potential. This result was backed up by more complete analyses which confirmed that the graviton propagator did indeed have the correct tensor structure, and that the effect of the extra dimension was to introduce a $1/r^3$ correction to the gravitational potential [6]:

$$V(r) = \frac{G_N}{r} \left(1 + \frac{2}{3} \frac{l^2}{r^2} \right). \quad (1)$$

An elegant description of nonperturbative gravity on the brane was provided by Shiromizu, Maeda and Sasaki [7]. Using a Gauss-Codazzi approach, they projected the 5D Einstein equations onto the brane to obtain the effective 4D field equations:

$$G_{\mu\nu} = \Lambda_4 g_{\mu\nu} + 8\pi G_N T_{\mu\nu} + \kappa^2 S_{\mu\nu} + \mathcal{E}_{\mu\nu}. \quad (2)$$

Here, Λ_4 is a residual cosmological constant on the brane and represents the mismatch between the brane tension and the negative bulk cosmological constant. $T_{\mu\nu}$ is the usual energy-momentum tensor of matter on the brane, and $S_{\mu\nu}(T^2)$ consists of squares of $T_{\mu\nu}$ and thus is a local, high energy correction term. $\mathcal{E}_{\mu\nu}$ consists of the projection of the bulk Weyl tensor onto the brane, and is nonlocal from the brane point of view. It is important to emphasize that since $\mathcal{E}_{\mu\nu}$ is not given in terms of data on the brane, the system of equations (2) is not closed, in general.

The generalization of the Friedmann-Robertson-Walker Universe that follows from Eq. (2) has been well explored [8]. The $S_{\mu\nu}$ term contributes a high energy correction term to the Friedmann equation, which is relevant only in the very early Universe, and the Weyl term contributes a “dark radiation” term. Hence, although all the implications may not have been calculated, braneworld cosmology for the pure RS scenario is pretty well understood. The situation for braneworld black holes (BBHs) is somewhat more complicated however, and there is no longer a simple solution [9,10]. Black holes are fascinating objects, and provide a potential testing ground for general relativity. It is therefore important to investigate braneworld generalizations of the Schwarzschild solution, and the possible observational signatures that could result.

The theory of gravitational lensing has been mostly developed in the weak field approximation, where it has been successful in explaining all observations [11]. However, one of the most spectacular consequences of the strong gravitational field surrounding a black hole is the large bending of light that can result for a light ray passing through this region. The study of strong gravita-

*Electronic address: r.s.whisker@dur.ac.uk

tional lensing was resurrected recently by Virbhadra and Ellis [12], who studied lensing by the galactic supermassive black hole, in an asymptotically flat background. Frittelli, Kling and Newman [13] found an exact lens equation without reference to a background metric and compared their results with those of Virbhadra and Ellis. In [14] Bozza *et al.* first defined a strong field limit and used it to investigate Schwarzschild black hole lensing analytically. This technique has been applied to Reissner-Nordström (RN) black holes [15] and the Gibbons-Maeda-Garfinkle-Horowitz-Strominger [16] charged black hole of heterotic string theory [17], and was generalized to an arbitrary static, spherically symmetric metric by Bozza [18]. In this paper we utilize this method to investigate the gravitational lensing properties of a couple of candidate BBH metrics.

Similar studies have been performed for a BBH with the induced geometry of the 5D Schwarzschild solution: $g_{tt} = g_{rr}^{-1} = 1 - r_h^2/r^2$. Both weak field lensing [19] and strong field lensing [20] for this geometry have been studied. However, this metric is only appropriate for black holes with a horizon size smaller than the AdS length scale of the extra dimension: $r_h < l \lesssim 0.1$ mm. Hence, this metric is not appropriate for investigating the phenomenology of massive astrophysical black holes.

II. BRANEWORLD BLACK HOLES

The general static, spherically symmetric metric on the brane can be written as

$$ds^2 = g_{\mu\nu} dx^\mu dx^\nu = A^2(r) dt^2 - B^2(r) dr^2 - C^2(r) d\Omega_{II}^2. \quad (3)$$

Clearly, this is not in the simplest gauge, as we can still choose our radial coordinate, r , quite arbitrarily. The vacuum brane field equations following from Eq. (2) (with Λ_4 set equal to zero) are

$$G_{\mu\nu} = \mathcal{E}_{\mu\nu}. \quad (4)$$

The solution of these equations requires the input of $\mathcal{E}_{\mu\nu}$ from the full 5D solution. In the absence of such a solution, an assumption about $\mathcal{E}_{\mu\nu}$ or $g_{\mu\nu}$ must be made in order to close the system of equations.

Several special solutions, making various assumptions about $g_{\mu\nu}$, have been presented in the literature. The first attempt at a BBH solution was the so-called black string solution of Chamblin *et al.* [9], which consists simply of the 4D Schwarzschild solution “stacked” into the extra dimension. Unfortunately, this solution has a singular AdS horizon and is unstable to classical perturbations [21]. The assumption $A^2 = 1/B^2$ leads to the tidal Reissner-Nordström solution of Dadhich *et al.* [22]:

$$ds^2 = \left(1 - \frac{2GM}{r} + \frac{Q}{r^2}\right) dt^2 - \left(1 - \frac{2GM}{r} + \frac{Q}{r^2}\right)^{-1} dr^2 - r^2 d\Omega_{II}^2. \quad (5)$$

Unlike the standard Reissner-Nordström solution, the “tidal charge” parameter Q can take both positive *and* negative values. Indeed, negative Q is the more natural since intuitively we would expect the tidal charge to *strengthen* the gravitational field, as it arises from the source mass M on the brane (see [22] for further discussion). This metric has the correct 5D ($\sim 1/r^2$) short distance behavior and so could be a good approximation in the strong field regime for small black holes. Solutions have also been found which assume a given form for the time or radial part of the metric [23,24]. Visser and Wiltshire [25] presented a more general method which generated an exact solution for a given radial metric form.

In all the above cases the radial gauge $C = r$ was chosen [although [25] did comment on how to use their method when $C(r)$ was not monotonic]. However, there are good reasons to believe that the area \mathcal{A} of the 2-spheres might not be monotonic. The second derivative of the area radius C (i.e. the radial function defined by $\sqrt{\mathcal{A}/4\pi}$) is given by

$$\frac{C''}{C} = -\frac{B^2}{2}(G'_t - G'_r) + \frac{C'}{C} \left(\frac{B'}{B} + \frac{A'}{A}\right). \quad (6)$$

Hence for the area function to be guaranteed to be monotonic we must have $G'_t - G'_r \geq 0$, which is equivalent to the dominant energy condition. While this is generally satisfied in standard Einstein gravity, it need not be in the case of extra dimensions, and so it is important for the exploration of BBHs that we do not make the restrictive ansatz $C = r$. (For a discussion of nonmonotonic radial functions in the context of braneworld *wormhole* solutions, see [26].)

An alternative to making guesses for the metric functions $g_{\mu\nu}$ is instead to make an assumption about the Weyl term $\mathcal{E}_{\mu\nu}$. Although $\mathcal{E}_{\mu\nu}$ is a complete unknown from the brane point of view, the symmetry of the problem allows it to be decomposed as [27]

$$\mathcal{E}_{\mu\nu} = \mathcal{U} \left(u_\mu u_\nu - \frac{1}{3} h_{\mu\nu} \right) + \Pi \left(r_\mu r_\nu + \frac{1}{3} h_{\mu\nu} \right), \quad (7)$$

where u^μ is a unit time vector and r^μ is a unit radial vector. Recently, we proposed a pragmatic approach to BBHs, in which an equation of state for the Weyl term is assumed [28] (see also [29]):

$$\Pi = \frac{\gamma - 1}{2} \mathcal{U}. \quad (8)$$

Of course, *a priori* there is no reason to suppose that the Weyl term should obey an equation of state. However, it is quite possible that it might have certain asymptotic equations of state which may be useful as near-horizon or long-range approximations to the (as yet unknown) exact solu-

tion. Using a dynamical systems approach, the system of equations (4) was solved, and the behavior of the solutions classified according to the equation of state parameter γ . It was found that asymptotically flat solutions require an equation of state $\gamma < 0$, and for $|\gamma| > 3$ the BBH solutions have a singular horizon, and are allowed both with and without turning points in the area function.

Using holography considerations, it was argued that we might expect equations of state with large γ to be relevant near the horizon. Taking this reasoning to its extreme, we proposed as a “working” metric for the near-horizon geometry the $\mathcal{U} = 0$ (i.e. $\gamma = \pm\infty$) solution:

$$ds^2 = \frac{(r - r_h)^2}{(r + r_t)^2} dt^2 - \frac{(r + r_t)^4}{r^4} dr^2 - \frac{(r + r_t)^4}{r^2} d\Omega_{II}^2, \quad (9)$$

which has a turning point in the area function at $r = r_t$, and the horizon at $r = r_h$ is singular (except for the special case $r_h = r_t$, which is just the standard Schwarzschild solution in isotropic coordinates). This metric has appeared in the area gauge as [23]

$$ds^2 = \left[(1 + \epsilon) \sqrt{1 - \frac{2GM}{R}} - \epsilon \right]^2 dt^2 - \left(1 - \frac{2GM}{R} \right)^{-1} dR^2 - R^2 d\Omega_{II}^2, \quad (10)$$

where $R = (r + r_t)^2/r$, $GM = 2r_t$ and $GM\epsilon = r_h - r_t$. For $\epsilon > 0$ this gauge is valid in the whole horizon exterior, however for $\epsilon < 0$ the turning point r_t is outside the horizon r_h and so the area gauge is inappropriate.

Although the choice of metric (9) is somewhat arbitrary, we believe that the horizon is likely to be singular and that a turning point in the area function is also likely, and this metric exhibits both these features. It has the added advantage of being analytic, and so seems a good choice for exploring these radical differences to the standard Schwarzschild geometry. In this paper we investigate the gravitational lensing properties of the metrics (5)¹ and (9), to see how braneworld effects might manifest themselves in observations of black holes.

It is important to emphasize that we envisage these only as possible near-horizon asymptotes of a more general metric, which has yet to be found. Neither metric satisfies the long distance $1/r^3$ correction to the gravitational potential, and both would be constrained in the weak field by the parametrized post-Newtonian observations.

III. GRAVITATIONAL LENSING

The lensing setup is shown in Fig. 1. Light emitted by the source S is deflected by the lens L and reaches the observer O at an angle θ to the optic axis OL , instead of β . The spacetime, described by the metric (3) centered on L ,

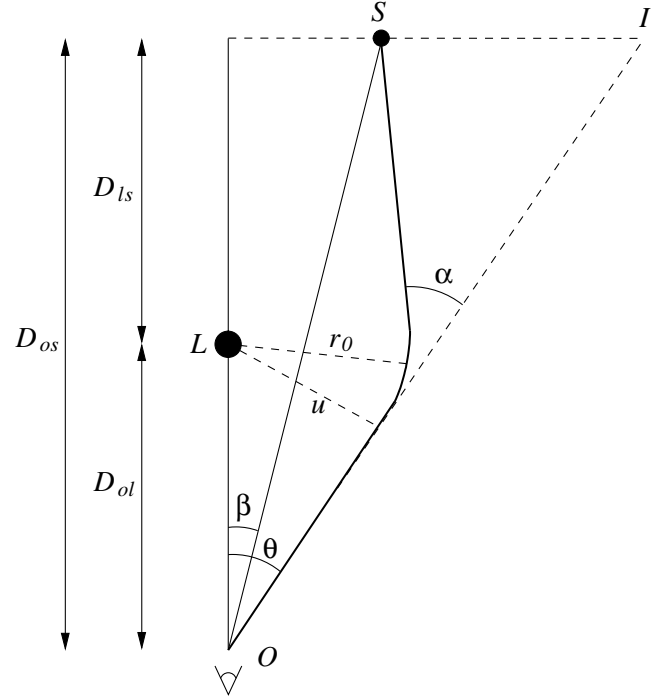


FIG. 1. Gravitational lensing diagram.

is asymptotically flat, and both observer and source are located in the flat region. By simple trigonometry, the lens equation can be written down:

$$\tan\beta = \tan\theta - \frac{D_{ls}}{D_{os}} [\tan\theta + \tan(\alpha - \theta)]. \quad (11)$$

From the null geodesic equations it is straightforward to show that the angular deflection of light as a function of radial distance from the lens is

$$\frac{d\phi}{dr} = \frac{B}{C\sqrt{u^2 A^2 - 1}}. \quad (12)$$

By conservation of angular momentum, the impact parameter u is given by

$$u = \frac{C_0}{A_0}, \quad (13)$$

where the subscript 0 indicates that the function is evaluated at the closest approach distance r_0 . Hence, the deflection angle is given by

$$\alpha(r_0) = I(r_0) - \pi = \int_{r_0}^{\infty} \frac{2B}{C} \left(\frac{C^2 A_0^2}{C_0^2 A^2} - 1 \right)^{-1/2} dr - \pi. \quad (14)$$

Equations (11) and (14) are the basic equations of gravitational lensing. In principle, the deflection angle α for a given metric can be calculated from Eq. (14). This can then be plugged into the lens equation (11), and the image position θ for a given source position β can be found.

¹In the context of the equation of state, (5) has $\gamma = -3$.

The theory of gravitational lensing has been developed mostly in the weak field limit, where several simplifying assumptions can be made. The angles in Eq. (11) are taken to be small, so that $\tan x$ can be replaced by x for $x = \beta, \theta, \alpha$, and the integrand in Eq. (14) is expanded to first order in the gravitational potential. For the Schwarzschild geometry, and setting $\beta = 0$, this leads to the well-known result:

$$\theta_E = \sqrt{\frac{4GM}{c^2} \frac{D_{ls}}{D_{os}D_{ol}}}, \quad (15)$$

where θ_E is the Einstein radius. In this formulation, general relativity has been successful in explaining all observations (see [11] for detailed reviews). However, it is important that gravitational lensing is not conceived of as a purely weak field phenomenon. Indeed, gravitational lensing in strong fields is one of the most promising tools for testing general relativity in its full, nonlinear form.

A. Strong field limit

As the impact parameter u of a light ray decreases, the deflection angle α increases as shown in Fig. 2. At some point, the deflection angle exceeds 2π and the photon performs a complete loop around the black hole before emerging. The images thus formed are termed ‘‘relativistic images’’ and a theoretically infinite number of such images are formed on either side of the lens, corresponding to successive winding numbers around the black hole. The photon sphere is the radius r_p at which a photon can unstably orbit the black hole, and is defined as the largest solution to the equation

$$\frac{A'(r)}{A(r)} = \frac{C'(r)}{C(r)}. \quad (16)$$

As r_0 approaches r_p , with corresponding impact parameter

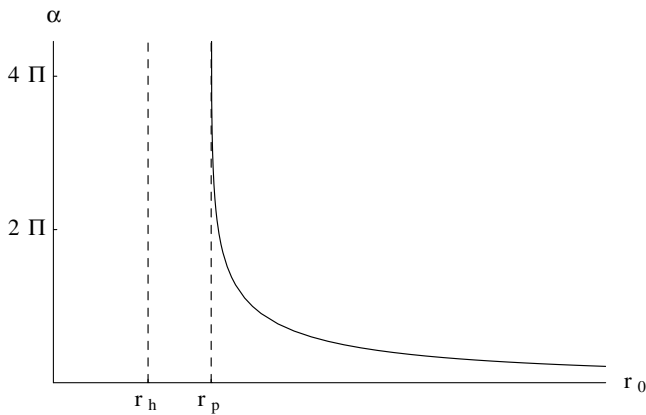


FIG. 2. General behavior of the deflection angle as a function of r_0 . As r_0 decreases, α increases, and each time it reaches a multiple of 2π the photon completes a loop around the black hole.

$$u_p = \frac{C_p}{A_p}, \quad (17)$$

the deflection angle diverges and for $r_0 < r_p$ the photon is captured by the black hole.

Bozza [18] has shown that this divergence is logarithmic for all spherically symmetric black hole metrics of the form (3). Hence the deflection angle can be expanded close to the divergence in the form

$$\alpha(r_0) = -a \ln\left(\frac{r_0}{r_p} - 1\right) + b + O(r_0 - r_p), \quad (18)$$

or in terms of the angular position of the image, $\theta = u/D_{ol}$,

$$\alpha(\theta) = -\bar{a} \ln\left(\frac{\theta D_{ol}}{u_p} - 1\right) + \bar{b} + O(u - u_p), \quad (19)$$

where the *strong field limit* (SFL) coefficients \bar{a} and \bar{b} depend on the metric functions evaluated at r_p . This formula allows a simple, analytic description of the relativistic images and their properties, rather than having to use the exact deflection angle calculated numerically from Eq. (14).

Equation (19) can be derived from Eq. (14) by splitting the integral into a divergent and nondivergent piece, and performing some expansions. Defining the new variable

$$z = \frac{A^2 - A_0^2}{1 - A_0^2}, \quad (20)$$

the integral in Eq. (14) becomes

$$I(r_0) = \int_0^1 R(z, r_0) f(z, r_0) dz, \quad (21)$$

where

$$R(z, r_0) = \frac{BC_0}{C^2 A'} (1 - A_0^2), \quad (22)$$

$$f(z, r_0) = \left(A_0^2 - [(1 - A_0^2)z + A_0^2] \frac{C_0^2}{C^2} \right)^{-1/2}. \quad (23)$$

The function $R(z, r_0)$ is regular for all values of z and r_0 , but $f(z, r_0)$ diverges for $z \rightarrow 0$. Expanding the argument of the square root in $f(z, r_0)$ to second order in z :

$$f(z, r_0) \sim f_0(z, r_0) = (m(r_0)z + n(r_0)z^2)^{-1/2}, \quad (24)$$

$$m(r_0) = \frac{A_0(1 - A_0^2)}{A_0'} \left(\frac{C_0'}{C_0} - \frac{A_0'}{A_0} \right), \quad (25)$$

$$n(r_0) = \frac{(1 - A_0^2)^2}{4A_0 A_0' C_0} \left[3C_0' \left(1 - \frac{A_0 C_0'}{A_0' C_0} \right) + \frac{A_0}{A_0'} \left(C_0'' - \frac{C_0' A_0''}{A_0'} \right) \right], \quad (26)$$

it is clear why the deflection angle diverges logarithmically for $r_0 = r_p$: with r_p given by Eq. (16), $m(r_p)$ vanishes.

Hence for $r_0 = r_p$, $f_0 \propto 1/z$ and the integral (21) diverges logarithmically.

Proceeding to split the integral (21) into a divergent and a regular piece, and performing further expansions (see [18] for the detailed derivation²), the SFL coefficients are obtained:

$$\bar{a} = \frac{R(0, r_p)}{2\sqrt{n_p}}, \quad (27)$$

$$\bar{b} = \bar{a} \ln \frac{2n_p}{A_p^2} + b_R - \pi, \quad (28)$$

where

$$n_p = n(r_p) = \frac{(1 - A_p^2)^2}{4C_p A_p^3} (C_p'' A_p' - C_p' A_p'') \quad (29)$$

and

$$b_R = \int_0^1 [R(z, r_p) f(z, r_p) - R(0, r_p) f_0(z, r_p)] dz, \quad (30)$$

is the integral $I(r_p)$ with the divergence subtracted.

IV. BRANEWORLD BLACK HOLE LENSING

In this section we apply the method outlined in the previous section to calculate the deflection angle in the strong field limit for the candidate BBH metrics (5) and (9) discussed in Sec. II.

A. $U = 0$ metric

The $U = 0$ metric (9) has a number of key differences to the standard Schwarzschild geometry; the horizon is singular, and the area function can have a turning point that lies either inside or outside the horizon. Another difference, due to the fact that $g_{tt} \neq g_{rr}^{-1}$, is that the Arnowitt-Deser-Misner (ADM) mass and gravitational mass (defined by g_{tt}) are no longer the same.

Normalizing the distances to $4r_t$ [which corresponds to a distance $2GM$ where M is the ADM mass—see Eq. (10)], the metric functions are

$$\begin{aligned} A^2(r) &= \frac{(r - r_h)^2}{(r + 1/4)^2}, & B^2(r) &= \frac{(r + 1/4)^4}{r^4}, \\ C^2(r) &= \frac{(r + 1/4)^4}{r^2}. \end{aligned} \quad (31)$$

The radius of the photon sphere is given by

$$r_p = \frac{1}{4} (1 + 4r_h + \sqrt{1 + 4r_h + 16r_h^2}). \quad (32)$$

The SFL coefficients \bar{a} , \bar{b} and u_p , calculated from

²Note: The expressions in [18] look slightly different to ours since we define the metric as $g_{\mu\nu} = \text{diag}(A^2, -B^2, -C^2)$ as opposed to $g_{\mu\nu} = \text{diag}(A, -B, -C)$ in [18].

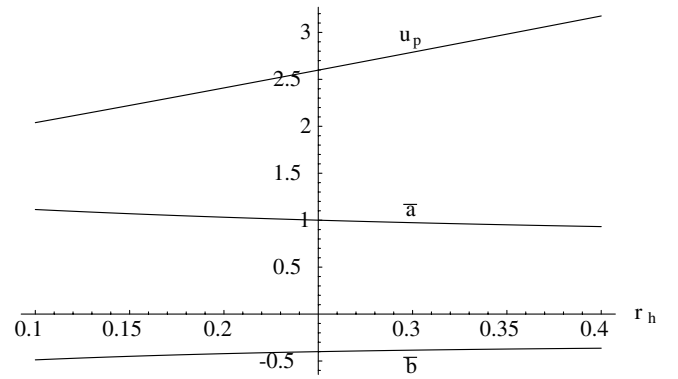


FIG. 3. SFL coefficients for the $U = 0$ metric (31), as functions of r_h . The standard Schwarzschild case is given by $r_h = 1/4$.

Eqs. (27), (28), and (17), are shown in Fig. 3. It can be seen that the biggest deviation from standard Schwarzschild lensing is for the minimum impact parameter u_p . This is because as the horizon is shifted inwards/outwards relative to the Schwarzschild case, the photon sphere is pulled/pushed along with it.

We can check the accuracy of the SFL approximation by comparing the exact deflection angle α_{exact} calculated from Eq. (14) with the SFL α_{SFL} from Eq. (19). The outermost relativistic image appears where $\alpha \simeq 2\pi$, which occurs for an impact parameter $u_1 = u_p + x$, where $x \sim 0.003$ depends on r_h . The discrepancy between $\alpha_{\text{exact}}(u_1)$ and $\alpha_{\text{SFL}}(u_1)$ is less than 0.13% for all values of r_h we consider. Hence, the SFL of the deflection angle is very accurate and can be reliably used to obtain accurate results for the properties of the relativistic images.

B. Tidal Reissner-Nordström metric

The tidal RN metric (5) has the same properties as the standard RN geometry for $q > 0$: there are two horizons, both of which lie within the Schwarzschild horizon, and the singularity at $r = 0$ is timelike. However, we can now have $q < 0$ in which case there is just one horizon, lying outside Schwarzschild, and the central singularity is spacelike, as in the Schwarzschild case. Normalizing the distances to $2GM$, with $q = Q/(2GM)^2$, the metric (5) becomes

$$\begin{aligned} A^2(r) &= 1 - \frac{1}{r} + \frac{q}{r^2}, & B^2(r) &= \left(1 - \frac{1}{r} + \frac{q}{r^2}\right)^{-1}, \\ C^2(r) &= r^2. \end{aligned} \quad (33)$$

The radius of the photon sphere is given by

$$r_p = \frac{1}{4} (3 + \sqrt{9 - 32q}). \quad (34)$$

The SFL coefficients are shown in Fig. 4. These results reproduce those of Eiroa *et al.* [15] for $q > 0$ (see also [18]), but we have extended the results to negative q . We

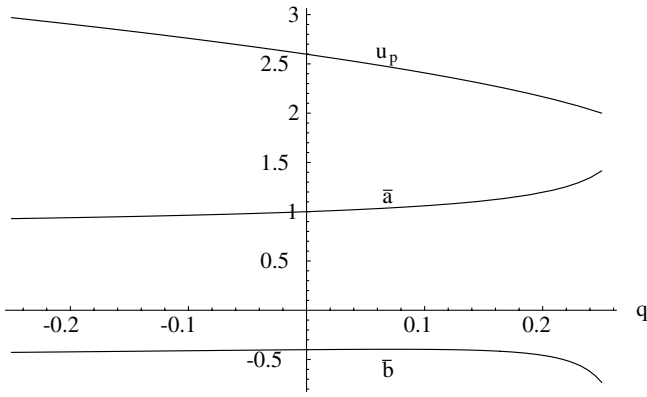


FIG. 4. SFL coefficients for the tidal Reissner-Nordström metric (33), as functions of q . The standard Schwarzschild case given by $q = 0$.

emphasize that there is *no* electric charge present for the tidal RN solution— q is a tidal charge parameter arising from the bulk Weyl tensor.

Again, comparing α_{exact} with α_{SFL} for an impact parameter corresponding to the outermost image, it is found that the discrepancy is less than 0.5% for the values of q considered here.

V. OBSERVABLES

In Sec. III A it was shown how to calculate the deflection angle in the strong field limit and in Sec. IV this method was applied to the candidate BBH metrics. In this section we put the SFL of the deflection angle into the lens equation to obtain analytic formulas for the properties of the relativistic images in terms of the SFL coefficients \bar{a} , \bar{b} and u_p .

As expected, the relativistic images formed by light rays winding around the black hole are greatly demagnified compared to the standard weak field images, and are most prominent when the source, lens and observer are highly aligned [12]. Hence, we restrict our attention to the case where β and θ are small (see [30] for the general case where this assumption is relaxed). Although we cannot assume α is small, if a light ray is going to reach the observer after winding around the black hole, α must be very close to a multiple of 2π . Writing $\alpha = 2n\pi + \Delta\alpha_n$, $n \in \mathbb{Z}$, the lens equation (11) becomes

$$\beta = \theta - \frac{D_{ls}}{D_{os}} \Delta\alpha_n. \quad (35)$$

First, we have to find the values θ_n^0 such that $\alpha(\theta_n^0) = 2n\pi$. With α given by Eq. (19) we find

$$\theta_n^0 = \frac{u_p}{D_{ol}} (1 + e_n), \quad (36)$$

where

$$e_n = e^{(\bar{b}-2n\pi)/\bar{a}}. \quad (37)$$

Thus the position of the n th relativistic image can be approximated by [18]

$$\theta_n = \theta_n^0 + \frac{u_p e_n (\beta - \theta_n^0) D_{os}}{\bar{a} D_{ls} D_{ol}}, \quad (38)$$

where the correction to θ_n^0 is much smaller than θ_n^0 . Approximating the position of the images by θ_n^0 , the magnification of the n th relativistic image is given by

$$\mu_n = \frac{1}{(\beta/\theta)\partial\beta/\partial\theta} \Big|_{\theta_n^0} \simeq \frac{u_p^2 e_n (1 + e_n) D_{os}}{\bar{a} \beta D_{ol}^2 D_{ls}}. \quad (39)$$

Equations (38) and (39) relate the position and magnification of the relativistic images to the SFL coefficients. We now focus on the simplest situation, where only the outermost image θ_1 is resolved as a single image, with the remaining images packed together at $\theta_\infty = u_p/D_{ol}$. Therefore we define the observables

$$s = \theta_1 - \theta_\infty, \quad (40)$$

$$f = \frac{\mu_1}{\sum_{n=2}^{\infty} \mu_n}, \quad (41)$$

which are, respectively, the separation between the outermost image and the others, and the flux ratio between the outermost image and all the others. It is found that these simplify to [18]

$$s = \theta_\infty e^{(\bar{b}-2\pi)/\bar{a}}, \quad (42)$$

$$f = e^{2\pi/\bar{a}}. \quad (43)$$

These equations are easily inverted to give \bar{a} , \bar{b} and so if an observation were able to measure s , f and θ_∞ the SFL coefficients could be determined and the nature of the lensing black hole identified.

A. An example: The galactic supermassive black hole

It is believed that the center of our galaxy harbors a black hole of mass $M = 2.8 \times 10^6 M_\odot$ [31]. Taking $D_{ol} = 8.5$ kpc, Virbhadra and Ellis [12] studied the lensing of a background source by this black hole and found that the relativistic images are formed at about $17 \mu\text{arc sec}$ from the optic axis.

In Table I we estimate the observables θ_∞ , s , f defined in the previous section for the $U = 0$ and tidal RN BBH metrics, as well as the standard Schwarzschild metric. It is clear that the easiest observable to resolve is θ_∞ , since a microarcsecond resolution is in principle attainable by VLBI projects such as MAXIM [32] and ARISE [33]. However, the disturbances inherent in such observations would make the identification of the faint relativistic images very difficult, as discussed in [12].

TABLE I. Estimates for the lensing observables for the central black hole of our galaxy. θ_∞ and s are defined in Sec. V, and $f_m = 2.5 \log f$ is f converted to magnitudes.

	$U = 0$						Tidal RN			
	Schwarzschild	$r_h = 0.1$	$r_h = 0.2$	$r_h = 0.3$	$r_h = 0.4$	$q = -0.2$	$q = -0.1$	$q = 0.1$	$q = 0.2$	
θ_∞ ($\mu\text{arc sec}$)	16.87	13.24	15.65	18.11	20.62	18.85	17.92	15.64	14.07	
s ($\mu\text{arc sec}$)	0.0211	0.0303	0.0235	0.0192	0.0164	0.0150	0.0173	0.0286	0.0502	
f_m (mags.)	6.82	6.13	6.61	7.01	7.32	7.26	7.08	6.44	5.70	

If a measurement of θ_∞ was made, it would be immediately capable of distinguishing between Schwarzschild and other types of geometry. However, to determine all the SFL coefficients and thus unambiguously identify the nature of the lensing black hole, it is necessary to also measure s and f . This would require the resolution of two extremely faint images separated by $\sim 0.02 \mu\text{arc sec}$. Such an observation in a realistic astrophysical environment is certainly not feasible in the near future, although if such an observation were ever possible, it would provide an excellent test of gravity in a strong field.

VI. CONCLUSIONS

Gravitational lensing in strong fields provides a potentially powerful tool for testing general relativity, and the strong field limit provides a useful framework for comparing lensing by different black hole metrics. Of the possible alternatives to standard general relativity, braneworld gravity is a very interesting model to explore given the current interest in theories with extra dimensions.

In this paper we have investigated strong field lensing by potential near-horizon BBH metrics. Although the correct BBH metric is unknown and much theoretical work remains to be done, this study is a useful first step to explore the possible effects that braneworlds could have on the spacetime surrounding a black hole.

Table I clearly shows that BBHs could have significantly different observational signatures than the standard Schwarzschild black hole. Although the resolutions required for these observations are beyond reach of current

observational facilities, this encourages the investigation of more realistically observable situations. An interesting possibility in this direction is the study of the accretion disks surrounding black holes.

The observed disk emission depends on several factors that could get modified by braneworld effects. A key factor is the radius of the innermost stable circular orbit, since emitting material at this radius sets the maximum temperature for the disk emission [34]. Just as the radius of the photon sphere is shifted inwards or outwards relative to the Schwarzschild case for a BBH, so too is the radius of the innermost stable orbit for matter [28]. In addition, the observed disk emission, and, in particular, the iron fluorescence line profile, is affected by relativistic effects [35] (doppler shift, gravitational redshift), which would be modified if the metric in the emitting region was not that of standard general relativity, but was a modified braneworld metric. Also, the light rays are gravitationally lensed by the central black hole as they escape the disk, and we have shown here that such lensing can be different from the Schwarzschild case for BBHs. In light of the results found here, it is not unreasonable to anticipate that these effects could result in distinctive observational signatures for accretion disks. This work is in progress.

ACKNOWLEDGMENTS

I would like to thank Ruth Gregory, Kris Beckwith, and Chris Done for helpful comments and suggestions. This work was supported by PPARC.

-
- [1] N. Arkani-Hamed, S. Dimopoulos, and G. R. Dvali, *Phys. Lett. B* **429**, 263 (1998); *Phys. Rev. D* **59**, 086004 (1999); I. Antoniadis, N. Arkani-Hamed, S. Dimopoulos, and G. R. Dvali, *Phys. Lett. B* **436**, 257 (1998).
 - [2] L. Randall and R. Sundrum, *Phys. Rev. Lett.* **83**, 3370 (1999); **83**, 4690 (1999).
 - [3] V. A. Rubakov and M. E. Shaposhnikov, *Phys. Lett.* **125B**, 136 (1983); **125B**, 139 (1983); K. Akama, *Lect. Notes Phys.* **176**, 267 (1982).
 - [4] R. Maartens, *Living Rev. Relativity* **7**, 7 (2004); P. Brax and C. van de Bruck, *Classical Quantum Gravity* **20**, R201 (2003); V. Rubakov, *Phys. Usp.* **44**, 871 (2001); D. Langlois, *Prog. Theor. Phys. Suppl.* **148**, 181 (2003).
 - [5] P. Horava and E. Witten, *Nucl. Phys.* **B475**, 94 (1996); A. Lukas, B. A. Ovrut, K. S. Stelle, and D. Waldram, *Phys. Rev. D* **59**, 086001 (1999).
 - [6] J. Garriga and T. Tanaka, *Phys. Rev. Lett.* **84**, 2778 (2000); S. B. Giddings, E. Katz, and L. Randall, *J. High Energy Phys.* 03 (2000) 023.
 - [7] T. Shiromizu, K. I. Maeda, and M. Sasaki, *Phys. Rev. D* **62**, 024012 (2000).

- [8] P. Binetruy, C. Deffayet, and D. Langlois, Nucl. Phys. **B565**, 269 (2000); C. Csaki, M. Graesser, C. F. Kolda, and J. Terning, Phys. Lett. B **462**, 34 (1999); J. M. Cline, C. Grojean, and G. Servant, Phys. Rev. Lett. **83**, 4245 (1999); P. Bowcock, C. Charmousis, and R. Gregory, Classical Quantum Gravity **17**, 4745 (2000).
- [9] A. Chamblin, S. W. Hawking, and H. S. Reall, Phys. Rev. D **61**, 065007 (2000).
- [10] T. Wiseman, Phys. Rev. D **65**, 124007 (2002); C. Charmousis and R. Gregory, Classical Quantum Gravity **21**, 527 (2004).
- [11] P. Schneider, J. Ehlers, and E. E. Falco, *Gravitational Lenses* (Springer-Verlag, Berlin, 1992); R. D. Blandford and R. Narayan, Annu. Rev. Astron. Astrophys. **30**, 311 (1992); R. Narayan and M. Bartelmann, astro-ph/9606001.
- [12] K. S. Virbhadra and G. F. R. Ellis, Phys. Rev. D **62**, 084003 (2000).
- [13] S. Frittelli, T. P. Kling, and E. T. Newman, Phys. Rev. D **61**, 064021 (2000).
- [14] V. Bozza, S. Capozziello, G. Iovane, and G. Scarpetta, Gen. Relativ. Gravit. **33**, 1535 (2001).
- [15] E. F. Eiroa, G. E. Romero, and D. F. Torres, Phys. Rev. D **66**, 024010 (2002).
- [16] G. W. Gibbons, Nucl. Phys. **B207**, 337 (1982); G. W. Gibbons and K. I. Maeda, Nucl. Phys. **B298**, 741 (1988); D. Garfinkle, G. T. Horowitz, and A. Strominger, Phys. Rev. D **43**, 3140 (1991); **45**, 3888(E) (1992).
- [17] A. Bhadra, Phys. Rev. D **67**, 103009 (2003).
- [18] V. Bozza, Phys. Rev. D **66**, 103001 (2002).
- [19] A. S. Majumdar and N. Mukherjee, astro-ph/0403405.
- [20] E. F. Eiroa, gr-qc/0410128.
- [21] R. Gregory, Classical Quantum Gravity **17**, L125 (2000).
- [22] N. Dadhich, R. Maartens, P. Papadopoulos, and V. Rezanian, Phys. Lett. B **487**, 1 (2000).
- [23] R. Casadio, A. Fabbri, and L. Mazzacurati, Phys. Rev. D **65**, 084040 (2002).
- [24] C. Germani and R. Maartens, Phys. Rev. D **64**, 124010 (2001).
- [25] M. Visser and D. L. Wiltshire, Phys. Rev. D **67**, 104004 (2003).
- [26] K. A. Bronnikov and S. W. Kim, Phys. Rev. D **67**, 064027 (2003); K. A. Bronnikov, V. N. Melnikov, and H. Dehnen, Phys. Rev. D **68**, 024025 (2003).
- [27] R. Maartens, Phys. Rev. D **62**, 084023 (2000).
- [28] R. Gregory, R. Whisker, K. Beckwith, and C. Done, J. Cosmol. Astropart. Phys. **10** (2004) 013.
- [29] T. Harko and M. K. Mak, Phys. Rev. D **69**, 064020 (2004).
- [30] V. Bozza and L. Mancini, Astrophys. J. **611**, 1045 (2004).
- [31] D. Richstone *et al.*, Nature (London) **395**, A14 (1998); F. Melia and H. Falcke, Annu. Rev. Astron. Astrophys. **39**, 309 (2001).
- [32] MAXIM web page: <http://maxim.gsfc.nasa.gov/>
- [33] J. S. Ulvestad, New Astron. Rev. **43**, 531 (1999).
- [34] N. I. Shakura and R. A. Sunyaev, Astron. Astrophys. **24**, 337 (1973); K. Ebisawa *et al.*, Astrophys. J. **403**, 684 (1993); A. Kubota and K. Makishima, Astrophys. J. **601**, 428 (2004); M. Gierlinski and C. Done, Mon. Not. R. Astron. Soc. **347**, 885 (2004).
- [35] C. T. Cunningham, Astrophys. J. **202**, 788 (1975); A. C. Fabian, K. Iwasawa, C. S. Reynolds, and A. J. Young, Publ. Astron. Soc. Pac. **112**, 1145 (2000).